

Modeling Low-Dose-Rate Effects in Irradiated Bipolar-Base Oxides

R.J. Graves¹, Member, IEEE, C.R. Cirba², R.D. Schrimpf², Fellow, IEEE, R.J. Milanowski², A. Michez³, D.M. Fleetwood⁴, Fellow, IEEE, S.C. Witczak⁵, Member, IEEE, and F. Saigne³,

¹SILVACO International, Scottsdale, Arizona 85251 USA

²Vanderbilt University, ECE Dept., Nashville, Tennessee 37235-1683 USA

³CEM2 Universite Montpellier II, 34095 Montpellier Cedex, FRANCE

⁴Sandia National Laboratories, Albuquerque, New Mexico 87185-1083 USA

⁵The Aerospace Corporation, Los Angeles, California 90009-9257 USA

Abstract

A physical model is developed to quantify the contribution of oxide-trapped charge to enhanced low-dose-rate gain degradation in bipolar junction transistors. Multiple-trapping simulations show that space charge limited transport is partially responsible for low-dose-rate enhancement. At low dose rates, more holes are trapped near the silicon-oxide interface than at high dose rates, resulting in larger midgap voltage shifts at lower dose rates. The additional trapped charge near the interface may cause an exponential increase in excess base current, and a resultant decrease in current gain for some NPN bipolar technologies.

I. INTRODUCTION

Bipolar junction transistors (BJTs) are used in modern integrated circuits because of their high speed and current-drive capability, low noise, and linearity. Bipolar technologies have evolved rapidly during the last decade, and modern polysilicon-emitter transistors (PETs) have emerged to overcome some of the traditional disadvantages of BJTs, offering lower power consumption, and higher packing densities [1]. PETs have been implemented in modern BiCMOS (Bipolar Complementary Metal-Oxide-Semiconductor) processes, using aggressive scaling techniques and modern fabrication processes such as ion implantation and high-temperature steps, which may increase the density of defects in silicon dioxide films.

Recent studies of PETs in modern ICs have caused increased concern about radiation-induced current gain degradation, a primary failure mechanism for BJTs in analog circuits. Enhanced low-dose-rate sensitivity (ELDRS) of current gain degradation has been observed in these devices [2]; however, to date no verified physical models exist that fully explain ELDRS. Dose rate dependence has been studied

for several bipolar technologies, using individual devices [3-7] and integrated circuits [8,9]. Physical models have been proposed for enhanced current gain ($\beta = I_C/I_B$) degradation at low dose rates for both NPN [10] and PNP [7] transistors exposed to ionizing radiation. These models have been verified and extended, using charge separation methods [11] coupled with thermally stimulated current (TSC) and capacitance-voltage (C-V) MOS capacitor test results [12,13], to show that the low-dose-rate current gain degradation of advanced bipolar devices is sensitive to the quality of the relatively thick, ion-implanted, thermally grown, base-emitter screen oxide.

Current gain degradation in irradiated crystalline-emitter BJTs had been examined prior to the work in [2]. The primary degradation mechanism for crystalline-emitter BJTs was identified in [14] as increased excess base current ($\Delta I_B = I_B - I_{B0}$, where I_{B0} is the pre-irradiation base current) due to: (1) oxide-trapped-charge driven spread of the base-emitter depletion region, and (2) interface-trap driven increase in surface recombination velocity (SRV). While the effects of oxide trapped charge (N_{ox}) were initially considered secondary to the influence of interface traps (N_{it}), the advanced, process-damaged BJT oxides were recognized in [14] as possible sources of low-dose-rate gain degradation. If base-emitter oxides were sufficiently thick and damaged, then low internal electric fields due to oxide-trapped charge might dominate the electronic behavior of the base-emitter junction.

Wei, *et al.* identified oxide-trapped charge as the dominant feature in the radiation response of a specific NPN BJT technology, as shown in Figure 1 [6]. Note that $\Delta I_B \sim \exp(N_{ox}^2)$, for lower values of oxide-trapped charge density, and the saturation of ΔI_B for higher trapped charge values, after a critical transition value of N_{ox} . Note also that ΔI_B is higher for lower dose rates at equivalent levels of trapped charge, so the enhanced current gain degradation may also be caused in part by increased interface trap densities.

Oxide-trapped charge and interface traps interact differently in BJTs than in metal-oxide-semiconductor field-effect transistors (MOSFETs). In MOSFETs the effects of trapped oxide charge and interface traps are additive to first order, each contributing characteristic voltage shifts to the

This work is supported by the Defense Special Weapons Agency, Mission Research Corporation, Sandia National Laboratories, and The Aerospace Corporation. Sandia Labs is operated by the Sandia Corporation, a Lockheed Martin Company, for DOE under Contract No. DE-AC04-94AL85000. Work performed at The Aerospace Corporation is supported by Aerospace's IR&D Program.

DISCLAIMER

This report was prepared as an account of work sponsored by an agency of the United States Government. Neither the United States Government nor any agency thereof, nor any of their employees, make any warranty, express or implied, or assumes any legal liability or responsibility for the accuracy, completeness, or usefulness of any information, apparatus, product, or process disclosed, or represents that its use would not infringe privately owned rights. Reference herein to any specific commercial product, process, or service by trade name, trademark, manufacturer, or otherwise does not necessarily constitute or imply its endorsement, recommendation, or favoring by the United States Government or any agency thereof. The views and opinions of authors expressed herein do not necessarily state or reflect those of the United States Government or any agency thereof.

DISCLAIMER

**Portions of this document may be illegible
in electronic image products. Images are
produced from the best available original
document.**

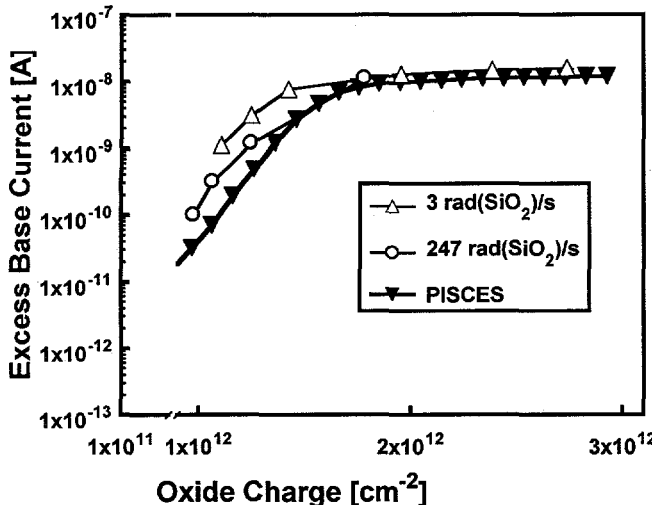


Figure 1. Excess base current vs. net oxide charge density from charge separation and PISCES simulation. Experimental data from NPN BJTs irradiated to 1 Mrad(SiO₂) total dose. After [6].

threshold voltage shift. The characteristic parameter for BJTs, however, is gain degradation, caused by the interactive effects of N_{ox} , N_{it} , and SRV. In this work we develop a model for dose-rate-dependent charge transport and trapping in irradiated bipolar-type MOS capacitor oxides, based on the studies of Fleetwood, *et al.* [12,13], which show higher midgap voltage shifts at lower dose rates, as illustrated in Figure 2. In addition, we model electron tunneling and compensation, since the TSC and C-V data of [12] and [13] suggest high (80-90%) rates of electron compensation in some irradiated thermal oxides. Though the focus of this work is oxide-trapped charge, space charge effects due to transporting holes are likely to affect interface trap formation as well, if the mechanism is related to proton release and transport.

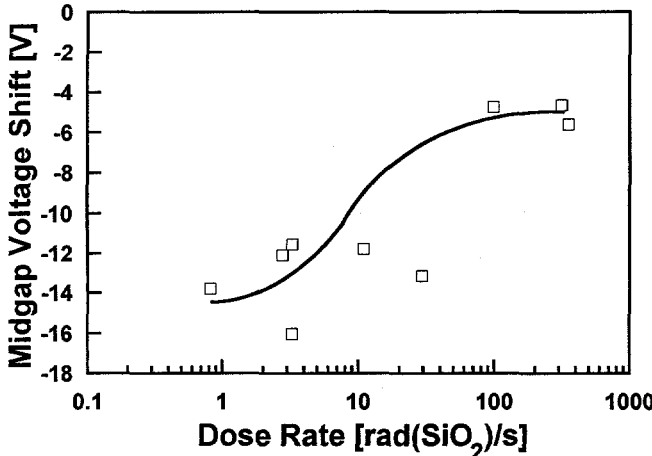


Figure 2. Experimental midgap voltage shift vs. dose rate for MOS capacitors with 600 nm wet thermal oxides on p-type substrates. Irradiation to 200 krad(SiO₂) total dose at room temperature using 10-keV x-rays at 0 V bias. After [13].

II. PHYSICAL MODEL

Time-dependent effects are reasonably well understood in MOS devices, and poorly understood in bipolar devices. This is because the currents in BJTs are functions of nonlinear, interactive effects of oxide-trapped charge and interface states, minority and majority carrier concentrations, recombination rates, and the surface potentials in sensitive regions of the device. Laboratory testing at low dose rates is inconvenient and expensive, thus the need for a more complete understanding of the physical mechanisms of ELDRS in BJTs. The MOS capacitor is a relatively simple structure, which allows us to model the major components of ELDRS due to surface potential and oxide/interface phenomena, and to compare predictions of the model with experimental data.

The MOS capacitor is modeled in one dimension using Poisson's equation, continuity equations, trap rate equations, current density equations, and empirical expressions for charge trapping, emission, and field-dependent hole yield. The model equations are based on the one-dimensional MOS capacitor structure shown in Figure 3. The results presented below are for specific parameter values and trap distributions. These values provide reasonable agreement with the experimental data considered here. Other choices for these parameters, however, may be used to model oxides with other properties.

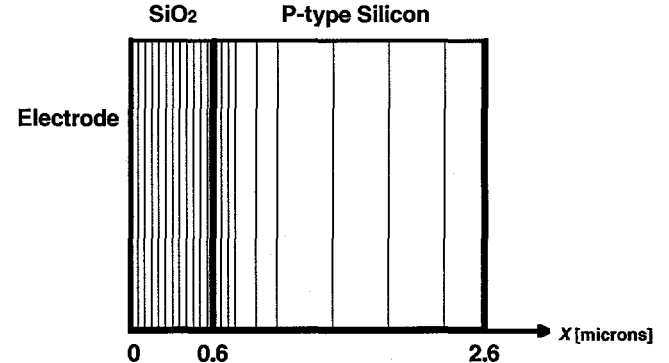


Figure 3. Schematic of spatially discretized, simulated 1-D MOS capacitor structure. The Si-SiO₂ interface is at 0.6 microns. There are approximately 100 points in the oxide at intervals (Δx) ranging from 20 nm in the oxide bulk to 0.2 nm near the interface region. Substrate doping is p-type, with a concentration of $3 \times 10^{16} \text{ cm}^{-3}$, and the work function at the electrode is 4.0 eV.

The physical mechanisms of the model are: (1) charge creation, (2) charge transport, (3) transport mediation via hole trapping and emission, and (4) electron compensation and tunneling.

A. Charge Creation

Carrier generation for the irradiated oxide is modeled as an electric-field-dependent process that results in a fractional hole yield, written as,

$$G_{ox} = Y(\mathcal{E}) \cdot G \quad (1)$$

where G is the nominal generation rate in SiO_2 , $(8.1 \times 10^{12} \text{ ehp/rad})$ [15,16], and $Y(\mathcal{E})$ is the field-dependent yield fraction given by [17-20],

$$Y(\mathcal{E}) = Y_0 + \left\{ \left[\frac{\mathcal{E}/\mathcal{E}_{\text{crit}}}{1 + \mathcal{E}/\mathcal{E}_{\text{crit}}} \right] \cdot (1 - Y_0) \right\} \quad (2)$$

where \mathcal{E} is the electric field at the oxide node, and $Y_0=0.36$, and $\mathcal{E}_{\text{crit}}=0.55$ are fitting parameters determined by experiment. Figure 4 shows a plot of the hole yield model compared to experimental data in [21].

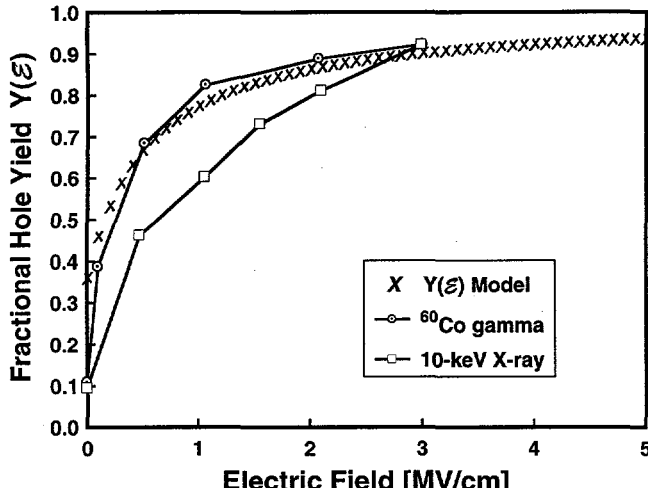


Figure 4. Measured fractional hole yield vs. applied positive electric field in thermal SiO_2 for ^{60}Co gamma ray and 10-keV x-ray irradiation. The hole yield function used in the model in this work is included. After [21].

B. Charge Transport, Trapping, and Emission

Carrier transport is modeled by drift-diffusion equations, mediated by trapping and emission at trap sites. We find that holes are the dominant carrier in the oxide bulk, due to the high intrinsic electron mobility in SiO_2 ($\sim 20 \text{ cm}^2/\text{V}\cdot\text{s}$) compared to the intrinsic mobility of holes ($\sim 10^{-5} \text{ cm}^2/\text{V}\cdot\text{s}$).

Hole trapping in the oxide is modeled using two different trap types. The first type is the deep trap, at 1.9 eV above the valence band, distributed spatially as a gaussian function with a maximum at the Si- SiO_2 interface. The second type is the shallow trap, at 1.0, 0.8, 0.7, and 0.65 eV above the valence band, distributed uniformly throughout the oxide. Dominant trap site characteristics are shown in Table 1.

Table 1.
Dominant oxide trap characteristics.

Distribution	Deep (gaussian)	Shallow (uniform)
E _a	1.9 eV	1.0, 0.8, 0.7, 0.65 eV
Peak Density	$2 \times 10^{17} \text{ cm}^{-3}$	1.0 eV: $1.8 \times 10^{16} \text{ cm}^{-3}$
Capture Cross-Section	$7.5 \times 10^{-14} \text{ cm}^{-2}$	$1.5 \times 10^{-13} \text{ cm}^{-2}$

Shallow hole trap sites capture a significant fraction of the radiation-induced holes, and re-emit them at characteristic time intervals, causing part of the hole population to move more slowly through the oxide. This transport-mediating quality of the shallow traps is crucial to the dose rate dependence of a low-quality thermal oxide, which likely has a large density of shallow traps distributed throughout the bulk.

Deep hole trap sites are assumed to be nearly permanent traps, and the holes trapped at deep sites are directly responsible for the midgap voltage shift, calculated from the model data as the first moment of charge with respect to the electrode,

$$\Delta V_{mg} = -\frac{1}{\varepsilon_{ox}} \int_0^L x \rho(x) dx \quad (3)$$

where $\rho(x)$ is the net charge density at each oxide gridpoint, x is the displacement from the electrode, and L is the total oxide depth.

Carriers are trapped and emitted at a characteristic rate, with coefficient t , written in the form,

$$t = \sigma \cdot \frac{J}{qp} \quad (4)$$

where σ is a constant capture cross-section, J is the instantaneous current density, q is the electronic charge, and p is the free carrier density. Note that the coefficient can also be interpreted as the product of the capture cross-section and the instantaneous carrier velocity.

Three forms of carrier emission appear in the model: (1) holes emitted from shallow trap sites, (2) holes emitted from deep trap sites, and (3) compensating electrons emitted from deep trap sites (discussed in the following section). The emission rate is inversely proportional to the carrier thermal lifetime, τ , given by the product of the attempt-to-escape frequency, and the exponential function of trap activation energy [23,24],

$$\frac{1}{\tau} = N_v \sigma v_{th} \cdot \exp\left(-\frac{E_a}{kT}\right) \quad (5)$$

where the first three terms constitute the attempt-to-escape frequency, E_a is the activation trap activation energy, and v_{th} is the carrier thermal velocity, taken to be 10^7 cm/s , the value for silicon.

C. Electron Compensation and Tunneling

Once a hole is trapped at a deep site, a compensating electron may be trapped by an adjacent oxygen atom, forming a dipole rather than directly recombining [12,13,22]. It is important to note that this compensating electron is modeled to be captured at existing deep-trapped hole, and emitted only when the hole is emitted. The compensation rate is modeled by a characteristic time coefficient of the same form as Equation 4.

The holes in deep traps near the Si-SiO₂ interface interact with electrons in the silicon valence band, resulting in a “tunneling front” model for electrons through the potential barrier, and compensation near the interface. We assume that recombination or annealing is not significant in modifying the midgap voltage shift (both carriers would be emitted to their respective bands), and write the tunneling probability $Z(t)$ [25] as,

$$Z(t) = \exp \left[-2 \int_0^t \frac{2m^*}{\hbar^2} (V(t) - E) \right]^{1/2} \quad (6)$$

where m^* is the electron effective mass, $V(t)$ is the potential barrier of the oxide for an electron in the silicon valence band, and E is the transfer energy which is zero for this tunneling model.

III. SIMULATION RESULTS

A multiple trapping-detrapping model (ACCES) is used to simulate charge transport and trapping in the MOS system. ACCES was developed at Universite Montpellier II, France [26,27], for studying hole trapping in the bird’s beak region of field oxides, and was modified at Vanderbilt University to focus on the problem of low-electric-field charge transport and trapping in bipolar screen oxides. This simulator also models electric-field-dependent electron-hole pair recombination, electron compensation, and electron tunneling at the Si-SiO₂ interface.

Simulations show that space charge limited transport is partially responsible for low-dose-rate enhancement of BJT current gain. The electric field in the oxide at high dose rate is significantly perturbed by a build-up of shallow-trapped oxide charge. This dose-rate-dependent electric field in turn causes a dose-rate dependent distribution of transporting and trapped oxide charge. More holes are trapped near the Si-SiO₂ interface at low dose rates than at high dose rates, resulting in a larger midgap voltage shift for low dose rates.

A. Deep-Trapped Hole Density and Midgap Voltage Shift

The key result for understanding the physical model is the density of holes trapped near the Si-SiO₂ interface. NPN devices exposed to ionizing radiation typically exhibit an increase in base current, and relatively constant collector current. The base current and therefore the current gain of a modern NPN BJT is quite sensitive to the surface potential, especially near the base-emitter junction. The simulator solutions show a larger density of deep-trapped holes in the oxide layer near the interface at low dose rates compared to high dose rates. This greater positive interface charge density at lower dose rates may lead to enhanced surface recombination in the lightly-doped p-type bases of NPN transistors, and in the p-type emitters of PNP devices [2-7,10-12,14].

Figure 5 is a plot of the oxide deep-trapped hole density within 20nm of the Si-SiO₂ interface. These deep-trapped holes are the direct source of N_{ox} and ΔV_{mg} in the model. The distributions of free and shallow-trapped carriers modify carrier transport by perturbing the electric field during irradiation, but the deep or permanently trapped holes are still present after irradiation, leading to a shift in the midgap voltage. The total dose for the simulations described in this work is 200 krad(SiO₂).

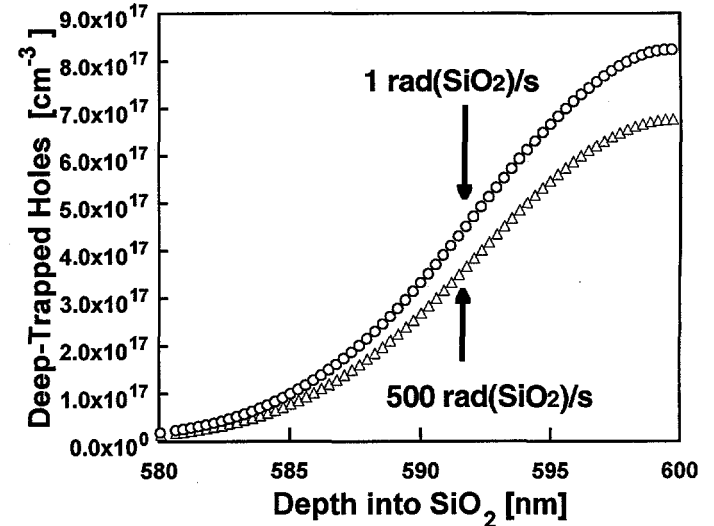


Figure 5. Density of holes in deep traps vs. oxide depth near the Si-SiO₂ interface, at two dose rates. The gate electrode is at 0 nm, not shown, and the interface is at 600 nm. Simulated irradiation to ~ 200 krad(SiO₂) at 0 V bias, 300 K.

The charge distribution of Figure 5 leads to a midgap voltage shift vs. dose rate plot shown in Figure 6, modified by some (peak ~ 38%) electron compensation of deep-trapped holes.

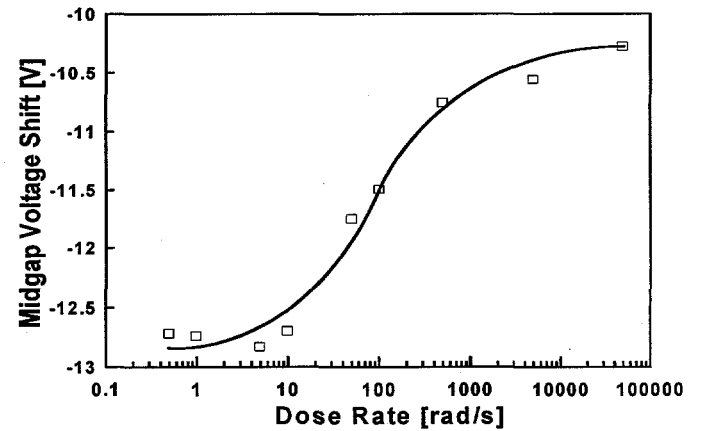


Figure 6. Simulated ΔV_{mg} vs. dose rate for 600 nm oxide in MOS capacitor structure. Note higher midgap voltage shift at lower dose rates. Simulated irradiation conditions are the same as in Figure 5.

Previous studies indicate that most (80-90%) of the deep trapped holes are compensated in some bipolar-type oxides [25,26]. The simulation result does not show this degree of compensation; however, the model accounts for electron

tunneling and compensation across the the Si-SiO₂ interface, where large numbers of holes are trapped. Uncertainties in physical parameters such as trap densities, distributions, and capture cross-sections may affect the solutions. We expect that for heavily process-damaged bipolar-base oxides, trap densities may be higher and differently distributed than those currently simulated. The trap capture cross-sections, for example, are approximated as constants (for numerical tractability) at a given energy level, although capture cross-sections are known to be electric-field dependent [21,28,29]. This field dependence may be the driving physical mechanism in the device, as we discuss next.

B. Oxide Electric Field and Dose-Rate Dependence of Trapped Charge

Except at low electric fields, a large fraction of the ionizing-radiation-induced charge is available to transport under the influence of the electric field. This means that at low fields, fewer electron-hole pairs survive the initial recombination process, and those that do will transport slower ($\sim \mu E$) than those at higher fields. It follows, then, that the charge transport properties of the oxide may exhibit wide spatial variation due to changes in field-dependent parameters such as capture cross section or hole yield, and well as local trap densities. Figure 7 shows a plot of the electric field vs. depth into the oxide for a 200 krad(SiO₂) total dose exposure at both high and low dose rate cases. For the low dose rate (1 rad(SiO₂)/s) case, the field is small, constant and positive throughout the oxide bulk, so generated holes tend to move toward the Si-SiO₂ interface. Both high and low dose rate cases show perturbation of the field near the interface due to the net positive charge (N_{ox}) located in deep traps. Note the field reversal near the oxide midpoint for the high dose rate (500 rad(SiO₂)/s) simulation, confirming the models for space charge limited transport in previous work [12,13].

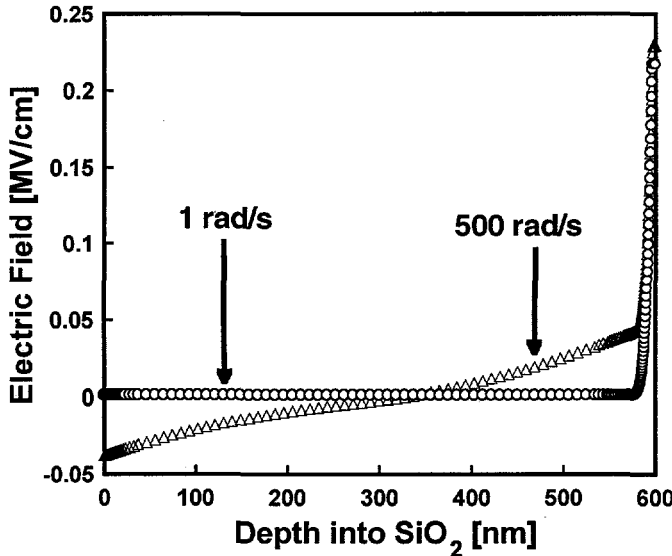


Figure 7. Simulated electric field vs. depth into oxide, at two dose rates. The electrode is at the origin. Simulated irradiation conditions are the same as in Figures 5 and 6.

This situation is further illustrated in Figure 8, for an oxide with a uniform charge distribution. the electric field comes directly from Poisson's equation. At high dose rates, there is a relatively large density of transporting holes in the oxide, mediated by shallow trap energy levels. This hole density increases the slope of the internal electric field, causing field reversal for sufficiently large charge densities.

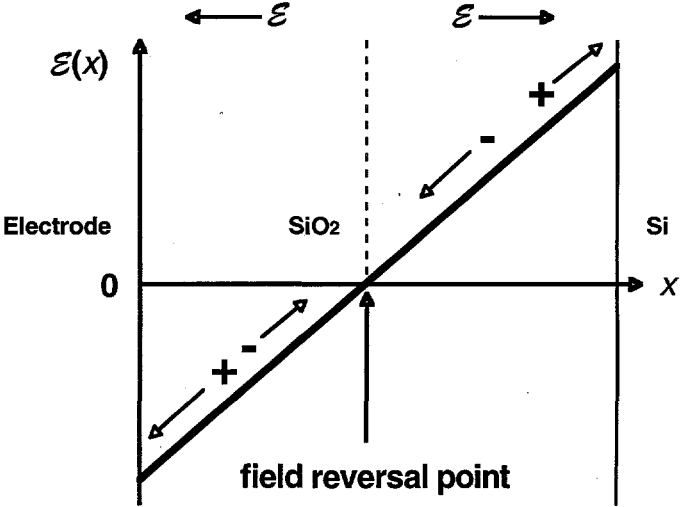


Figure 8. Schematic of oxide electric field, for a uniform distribution of holes in the space charge limited transport condition. Field directions, reversal point, and carrier drift directions are shown.

The electric field plots in Figures 7 and 8 are characteristic of previous studies [12,13,30] which identify space charge limited transport as a dominant effect at dose rates high enough to cause significant oxide charging, electric field reversal, and a resultant low field region in the oxide bulk. The space charge limited transport condition reduces hole yield (Figure 4), and may provide an extended domain for trapping and compensation events to occur more frequently, thus slowing hole transport even more and increasing the fraction of compensated holes in the oxide bulk.

Next we consider the dose required to induce the space charge limited transport condition illustrated in Figure 8. As positive charge builds up in the oxide, we define two limiting cases with respect to the characteristic time for hole charge build-up (τ_g), and the characteristic time for hole transport across the oxide (τ_h) [13]. For $\tau_h \ll \tau_g$, the low-dose-rate case, holes transport faster than they build up in the oxide bulk and become trapped near the Si-SiO₂ interface, where high densities of deep trap sites exist. For $\tau_h \geq \tau_g$, the high-dose-rate case, holes build up faster than they are transported out of the oxide, causing the electric field in the bulk to reverse (see Figures 7,8), reducing the number of holes that transport to the interface compared to the low-dose-rate case. This simplified analysis of the mediated transport is a useful concept that appears to be justified by the different saturation values of ΔV_{mg} observed at high and low dose rates in the simulation results of Figure 6. Note also the similarity in trends between the simulated midgap voltage shifts in Figure 6 and the

experimental MOS capacitor ΔV_{mg} vs. dose rate shown in Figure 2. The two differ significantly in the magnitude of the change in midgap voltage shift (~ 2.5 V simulated vs. ~ 10 V experimental), and differ moderately in the range of dose rates over which the transition occurs, but show qualitative agreement with the proposed physical mechanisms of [12] and [13]. We will show that the range of dose rates at which the transition occurs shifts with changes in trap energy levels, so the trends of the data are more important than the selected values for the physical parameters. The choice of parameter values appears to be physically reasonable, however, since the trends of simulated and experimental midgap voltage shift are similar.

Fleetwood, *et al.*, calculate the critical dose required to induce a -1 V shift in a 600 nm oxide which would lead to space charge limited transport ($D_{crit} \sim 0.7$ krad(SiO₂)) [13]. This dose is much less than the doses at which ELDRS has been reported [2,3,8,9,14], so the proposed space charge limited transport model gives results, which are consistent with a candidate mechanism for ELDRS.

Note also that the charge state of defect sites has its greatest effect on midgap voltage shift when furthest from the electrode, that is, just at the interface, so further work on tunneling and compensation appears to be warranted.

After an initial transient time, which can vary with oxide quality and dose rate from $\sim 10^2$ - 10^5 s, the density of transporting holes in the 1.0 eV shallow traps dominates the field and current characteristics in the oxide bulk, as shown in Figure 9. The density of holes trapped at the 1.0 eV energy level is much larger than the density of holes trapped at the other three shallow trap levels (0.8, 0.7, and 0.65 eV). The shallower hole traps are introduced in the simulation to more accurately model dispersive transport in SiO₂.

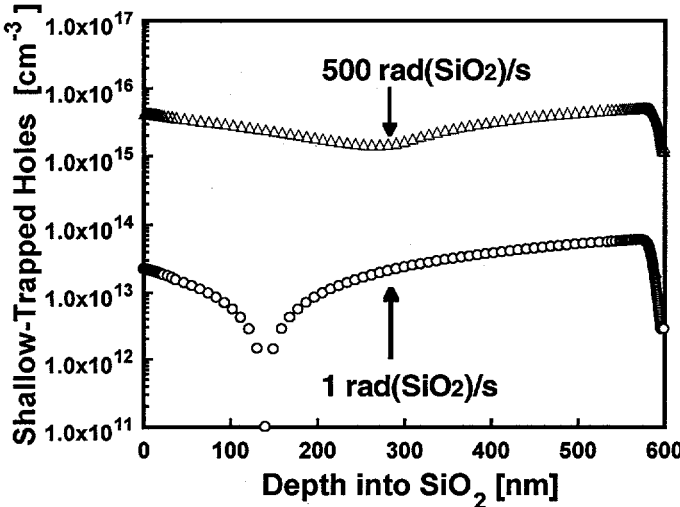


Figure 9. Simulated shallow-trap hole density vs. oxide depth at two dose rates. Irradiation conditions are the same as in Figures 5-7.

Note that the deep-trapped hole density in the oxide is quite small except for the interfacial region (Figure 5), and the free hole density shown in Figure 10 is negligible compared to the shallow-trapped holes throughout the oxide in Figure 9.

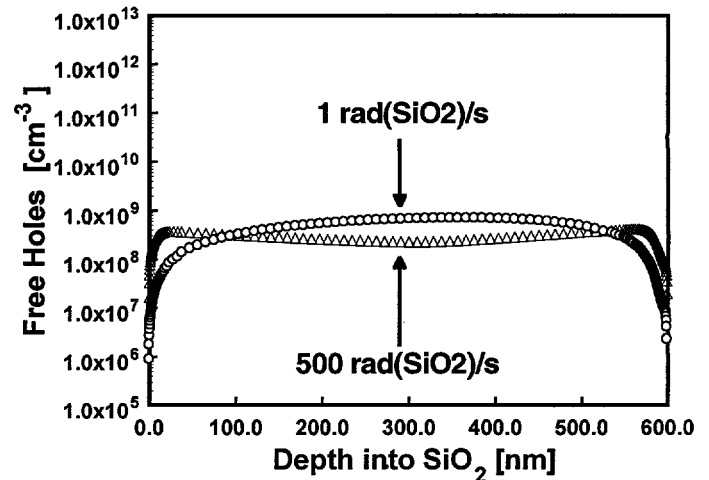


Figure 10. Simulated free hole density vs. oxide depth at two dose rates. Irradiation conditions are the same as in Figures 5-7, 9.

C. Temperature and Bias Dependence

The consistency of the model was checked by simulating the temperature and bias dependence of ΔV_{mg} vs. dose rate. For irradiation at high dose rate and high temperature, the resulting ΔV_{mg} is the same as that obtained at low dose rates and room temperature, as shown in Figure 11. This simulation was done using a single 1.0 eV shallow trap, without interface tunneling. The result is due to more rapid detrapping of holes from the shallow traps, so that that space charge does not alter the midgap voltage shift at high dose rates and high temperature.

Application of 3V positive bias to the MOS capacitor during irradiation is also sufficient to eliminate the dose-rate dependence of the charge transport, also shown in Figure 11. The result is consistent with experimental trends which show that the enhanced low-dose-rate effect is maximum for low oxide fields.

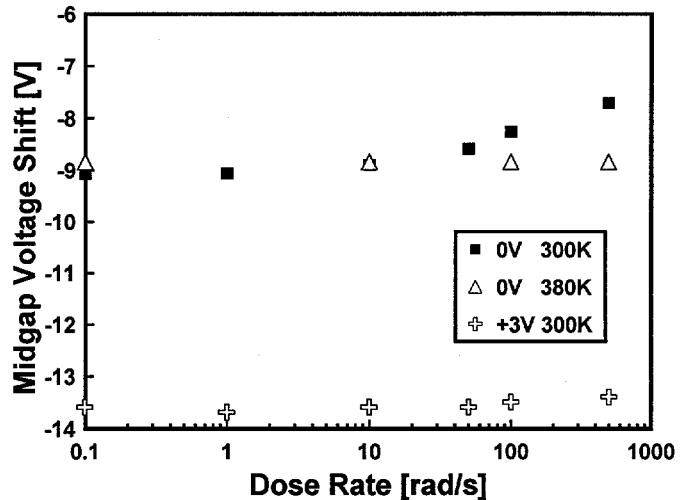


Figure 11. Simulated ΔV_{mg} vs. dose rate for high temperature and positive bias conditions. Irradiation conditions are the same as in Figures 5-7, 9, 10.

D. Shallow Trap Energy Variation

A test of the model was performed to determine the effect of changing shallow trap activation energy on midgap voltage shift, keeping the shallow trap spatial distribution (again using a single 1.0 eV trap energy) the same, and the deep trap activation energy and distribution the same. We would expect that, since the carrier emission times are exponential functions of the activation energy (Equation 5), a shallow hole trap with larger activation energy (further from the valence band) would give longer lifetimes for shallow trapped holes. We would then expect oxide charge to build up more quickly than it is transported, causing space charge effects to occur at lower dose rates. This effect is shown clearly in Figure 12. Note the smaller midgap voltage shift for this simulation with a single shallow trap energy and no interface tunneling model compared to the model of Figure 6.

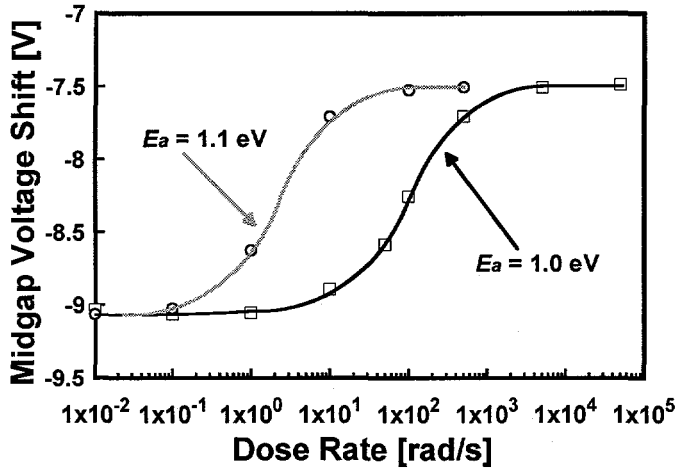


Figure 12. Simulated ΔV_{mg} vs. dose rate at two shallow trap activation energies. Note that the deeper shallow trap causes space charge effects at lower dose rates. Irradiation conditions are the same as in Figures 5-7, and 9-11.

The midgap voltage shift at (200 krad(SiO_2)) total dose, for the limiting cases of $\tau_h \ll \tau_g$ (low dose rate) or $\tau_h \geq \tau_g$ (high dose rate) should remain fixed by the density and distribution of deep trap sites, where the holes are permanently trapped. Figure 12 shows confirmation of this prediction.

IV. CONCLUSIONS

A physical model is developed to quantify the contribution of oxide-trapped charge to enhanced low-dose-rate gain degradation of advanced BJTs. Simulation of a MOS capacitor structure with oxide trap activation energies similar to bipolar-base oxides shows that space charge limited transport, characterized by a reversal of the electric field direction in the oxide bulk, is partially responsible for low-dose-rate enhancement.

Radiation-induced hole transport in the SiO_2 layer of an MOS capacitor is modeled in one dimension by drift-diffusion, mediated by the presence of shallow and deep traps associated with oxide defects. Holes trapped at shallow energy levels dominate the transport characteristics in the bulk of the oxide,

while holes trapped at deep energy levels become permanently trapped and are the source of the midgap voltage shift. We show that in the low dose rate case, more holes are trapped near the Si- SiO_2 interface compared to the high dose rate case, resulting in a larger midgap voltage shift for low dose rates. For BJTs operating in the regime where excess base current scales as $\exp(N_{ox}^2)$, the increased interfacial charge may result in relatively large increases in base current and gain degradation.

Carrier trapping and transport simulation is based on the multiple trapping model, a numerically tractable approach to modeling carrier transport in amorphous and vitreous structures such as SiO_2 , which do not have well-defined Fermi levels, but do exhibit measurable, wide energy bandgaps, and large differences in intrinsic hole and electron mobilities.

An important comparison made in the analysis of dose rate dependence in the simulations is the time required to build up space charge in the oxide bulk (τ_g) vs. the time required for holes to transport across the oxide via drift-diffusion and trapping (τ_h). These characteristic times define limiting cases for low dose rate and high dose rate conditions in the oxide, and are used to interpret the dose rate dependence of midgap voltage shift, and the space charge limited hole transport condition.

V. REFERENCES

- [1] C.R. Selvakumar, "Theoretical and Experimental Aspects of Polysilicon Emitter Bipolar Transistors," in *Polysilicon Emitter Bipolar Transistors*, ed. A.K. Kapoor and D.J. Roulston, IEEE Press, p. 3, 1989.
- [2] E.W. Enlow, R.L. Pease, W.E. Combs, R.D. Schrimpf, and R.N. Nowlin, "Response of Advanced Bipolar Processes to Ionizing Radiation," *IEEE Trans. Nucl. Sci.*, vol. 38, pp. 1342-1351, 1991.
- [3] R.N. Nowlin, E.W. Enlow, R.D. Schrimpf, and W.E. Combs, "Trends in the Total-Dose Response of Modern Bipolar Transistors," *IEEE Trans. Nucl. Sci.*, vol. 39, pp. 2026-2035, 1992.
- [4] R.N. Nowlin, D.M. Fleetwood, and R.D. Schrimpf, "Saturation of the Dose-Rate Response of BJTs Below 10 rad(SiO_2)/s: Implications for Hardness Assurance," *IEEE Trans. Nucl. Sci.*, vol. 41, pp. 2637-2641, 1994.
- [5] S.L. Kosier, W.E. Combs, A. Wei, R.D. Schrimpf, D.M. Fleetwood, M. DeLaus, and R.L. Pease, "Bounding the Total-Dose Response of Modern Bipolar Transistors," *IEEE Trans. Nucl. Sci.*, vol. 41, pp. 1864-1870, 1994.
- [6] A. Wei, S.L. Kosier, R.D. Schrimpf, D.M. Fleetwood, and W.E. Combs, "Dose-Rate Effects on Radiation-Induced Bipolar Junction Transistor Gain Degradation," *Appl. Phys. Lett.*, vol. 65, pp. 1918-1920, 1994.

[7] D.M. Schmidt, D.M. Fleetwood, R.D. Schrimpf, R.L. Pease, R.J. Graves, G.H. Johnson, K.F. Galloway, and W.E. Combs, "Comparison of Ionizing Radiation Induced Gain Degradation in Lateral, Substrate, and Vertical PNP BJTs," *IEEE Trans. Nucl. Sci.*, vol. 42, pp. 1541-1549, 1995.

[8] S. McClure, R.L. Pease, W. Will, and G. Perry, "Dependence of Total Dose Response of Bipolar Linear Microcircuits on Applied Dose Rate," *IEEE Trans. Nucl. Sci.*, vol. 41, pp. 2544-2549, 1994.

[9] A.H. Johnston, G.M. Swift, and B.G. Rax, "Total Dose Effects in Conventional Bipolar Transistors and Linear Integrated Circuits," *IEEE Trans. Nucl. Sci.*, vol. 41, pp. 2427-2436, 1994.

[10] S.L. Kosier, A. Wei, R.D. Schrimpf, D.M. Fleetwood, M. DeLaus, R.L. Pease, and W.E. Combs, "Physically Based Comparison of Hot-Carrier-Induced and Ionizing-Radiation Induced Degradation in BJTs," *IEEE Trans. Electron Devices*, vol. 42, pp. 436-444, 1995.

[11] S.L. Kosier, R.D. Schrimpf, R.N. Nowlin, D.M. Fleetwood, M. DeLaus, R.L. Pease, W.E. Combs, A. Wei, and F. Chai, "Charge Separation for Bipolar Transistors," *IEEE Trans. Nucl. Sci.*, vol. 41, pp. 1276-1285, 1993.

[12] D.M. Fleetwood, S.L. Kosier, R.N. Nowlin, R.D. Schrimpf, R.A. Reber, Jr., M. DeLaus, P.S. Winokur, A. Wei, W.E. Combs, and R.L. Pease, "Physical Mechanisms Contributing to Enhanced Bipolar Gain Degradation at Low Dose Rates," *IEEE Trans. Nucl. Sci.*, vol. 41, pp. 1871-1883, 1994.

[13] D.M. Fleetwood, L.C. Riewe, J.R. Schwank, S.C. Witczak, and R.D. Schrimpf, "Radiation Effects at Low Electric Fields in Thermal, SIMOX, and Bipolar-Base Oxides," *IEEE Trans. Nucl. Sci.*, vol. 43, pp. 2537-2546, 1996.

[14] A. Hart, J. Smyth, V. van Lint, D. Snowden, and R. Leadon, "Hardness Assurance Considerations for Long-Term Radiation Effects on Bipolar Structures," *IEEE Trans. Nucl. Sci.*, vol. 25, pp. 1502-1507, 1978.

[15] J.P. Mitchell, "Radiation-Induced Space Charge Buildup in MOS Structures," *IEEE Trans. Electron Dev.*, vol. 14, pp. 764-774, 1967.

[16] G.A. Ausman, Jr. and F.B. McLean, "Electron-Hole Pair Creation Energy in SiO₂," *Appl. Phys. Lett.*, vol. 26, pp. 173-175, 1975.

[17] G.A. Ausman, "Field Dependence of Geminate Recombination in a Dielectric Medium," *Harry Diamond Laboratories*, Report No. 2097, Adelphi, MD, 1986.

[18] H.E. Boesch, Jr. and J.M. McGarry, "Charge Yield and Dose Effects in MOS Capacitors at 80 K," *IEEE Trans. Nucl. Sci.*, vol. 23, pp. 1520-1525, 1976.

[19] C.M. Dozier, D.M. Fleetwood, D.B. Brown, and P.S. Winokur, "An Evaluation of Low-Energy X-Ray and Cobalt-60 Irradiations of MOS Transistors," *IEEE Trans. Nucl. Sci.*, vol. 34, pp. 1535-1539, 1987.

[20] J-L. Leray, "Contribution a l'étude des phénomènes induits par les Rayonnements Ionisants dans les Structures a Effect de Champ au Silicium ou a L'arseniure de Gallium Utilisees en Micro-Electronique," *These*, University de Paris-Sud Centre d'Orsay, 1989.

[21] F.B. McLean, H.E. Boesch, Jr., and T.R. Oldham, "Electron-Hole Generation, Transport, and Trapping in SiO₂," in *Ionizing Radiation Effects in MOS Devices and Circuits*, ed. T.P. Ma and P.V. Dressendorfer, John Wiley & Sons, New York, pp. 87-192, 1989.

[22] T.R. Oldham, A.J. Lelis, and F.B. McLean, "Spatial Dependence of Trapped Holes Determined from Tunneling Analysis and Measured Annealing," *IEEE Trans. Nucl. Sci.*, vol. 33, pp. 1203-1209, 1986.

[23] D.M. Fleetwood, S.L. Miller, R.A. Reber, Jr., P.J. McWhorter, P.S. Winokur, M.R. Shaneyfelt, and J.R. Schwank, "New Insights Into Radiation-Induced Oxide-Trap Charge Through Thermally-Stimulated-Current Measurement and Analysis," *IEEE Trans. Nucl. Sci.*, vol. 39, pp. 2192-2203, 1992.

[24] F. Saigne, L. Dusseau, J. Fesquet, J. Gasiot, R. Ecoffet, J.P. David, R.D. Schrimpf, and K.F. Galloway, "Experimental Validation of an Accelerated Method of Oxide-Trap-Level Characterization for Predicting Long Term Thermal Effects of Metal Oxide Semiconductor Devices," *IEEE Trans. Nucl. Sci.*, vol. 44, pp. 2001-2006, 1997.

[25] P.J. McWhorter, S.L. Miller, and W.M. Miller, "Modeling the Anneal of Radiation-Induced Trapped Holes in a Varying Thermal Environment," *IEEE Trans. Nucl. Sci.*, vol. 37, pp. 1682-1688, 1990.

[26] R. Escoffier, A. Michez, C. Cirba, G. Bordure, P. Paillet, V. Ferlet-Cavrois, and J-L. Leray, "Radiation Induced Shift Study in Parasitic MOS Structures by 2D Numerical Simulation," *RADECS*, pp. 45-49, 1995.

[27] C. Cirba, "Simulation Numerique du Piégeage et du Dépiégeage dans les Oxydes de Composants MOS," *These*, Université Montpellier II, 1995.

[28] T.H. Ning, "Capture Cross Section and Trap Concentration of Holes in Silicon Dioxide," *J. Appl. Phys.*, vol. 47, pp. 1079-1081, 1976.

[29] J.J. Tzou, J.Y.C. Sun, and C.T. Sah, "Field Dependence of Two Large Hole Capture Cross Sections in Thermal Oxide on Silicon," *Appl. Phys. Lett.*, vol. 43, pp. 861-863, 1983.

[30] D.M. Fleetwood, S.L. Miller, R.A. Reber, Jr., P.J. McWhorter, P.S. Winokur, M.R. Shaneyfelt, and J.R. Schwank, "New Insights Into Radiation-Induced Oxide-Trap Charge Through Thermally-Stimulated-Current Measurement and Analysis," *IEEE Trans. Nucl. Sci.*, vol. 39, pp. 2192-2203, 1992.